nature communications

Article

https://doi.org/10.1038/s41467-025-59037-1

Reaching the pinnacle of high-capacity optical transmission using a standard cladding diameter coupled-core multi-core fiber

Received: 11 September 2024

Accepted: 4 April 2025

Published online: 23 April 2025

Check for updates

Menno van den Hout[1,2] ✉, Ruben S. Luís[1], Benjamin J. Puttnam[1], Giammarco Di Sciullo[1,3], Tetsuya Hayashi[4], Ayumi Inoue[4], Takuji Nagashima[4], Simon Gross[5], Andrew Ross-Adams[6], Michael J. Withford[6], Lauren Dallachiesa[7], Nicolas K. Fontaine[7], Roland Ryf[7], Mikael Mazur[7], Haoshuo Chen[7], Jun Sakaguchi[1], Cristian Antonelli[3], Chigo Okonkwo[2], Hideaki Furukawa[1] & Georg Rademacher[1,8]

Data rates in optical networks have grown exponentially in recent decades and are expected to grow beyond the fundamental limits of current standard single-mode fiber networks. As such, novel transmission technologies are required to sustain this growth, and space-division multiplexing provides the most promising candidate to scale the capacity of optical networks in a way that is also cost-effective. For fiber fabrication and deployment, it is highly beneficial to use fibers with a standard cladding diameter. Here we demonstrate petabit-per-second-class data transmission using a space-division multiplexing fiber that approaches the limits of spatial multiplexing whilst minimizing the required signal processing complexity. This is done by designing and fabricating a low-loss 19-core multi-core fiber with randomly-coupled cores, a standard cladding diameter, and supporting a wideband wavelength-division multiplexed signal. The resulting data rate of 1.7 petabit/s is the highest reported amongst standard cladding diameter multi-core fibers and is approximately more than an order of magnitude higher than is supported by currently deployed single-mode fibers, paving the way for next-generation ultra-fast optical transmission networks.

Current optical transmission systems based on single-mode fibers (SMFs) have enabled the exponential growth in Internet-driven traffic in recent decades[1]. However, as data traffic demand is increasing exponentially, SMF-based networks are approaching their fundamental capacity limits[2–7]. Previously, the capacity of SMF networks has been increased by exploiting the orthogonal multiplexing dimensions of an optical fiber, such as polarization and wavelength multiplexing. Space-division multiplexing (SDM)[8] employs the

[1]National Institute of Information and Communications Technology, Tokyo, Japan. [2]High-Capacity Optical Transmission Laboratory, Eindhoven University of Technology, Eindhoven, The Netherlands. [3]University of L'Aquila and CNIT, L'Aquila, Italy. [4]Sumitomo Electric Industries, Ltd., Yokohama, Japan. [5]MQ Photonics Research Centre, School of Engineering, Macquarie University, Sydney, NSW, Australia. [6]MQ Photonics Research Centre, School of Mathematical and Physical Sciences, Macquarie University, Sydney, NSW, Australia. [7]Nokia Bell Labs, Murray Hill, NJ, USA. [8]Institute of Electrical and Optical Communications, University of Stuttgart, Stuttgart, Germany. ✉e-mail: m.v.d.hout@tue.nl

https://doi.org/10.1038/s41467-025-59037-1

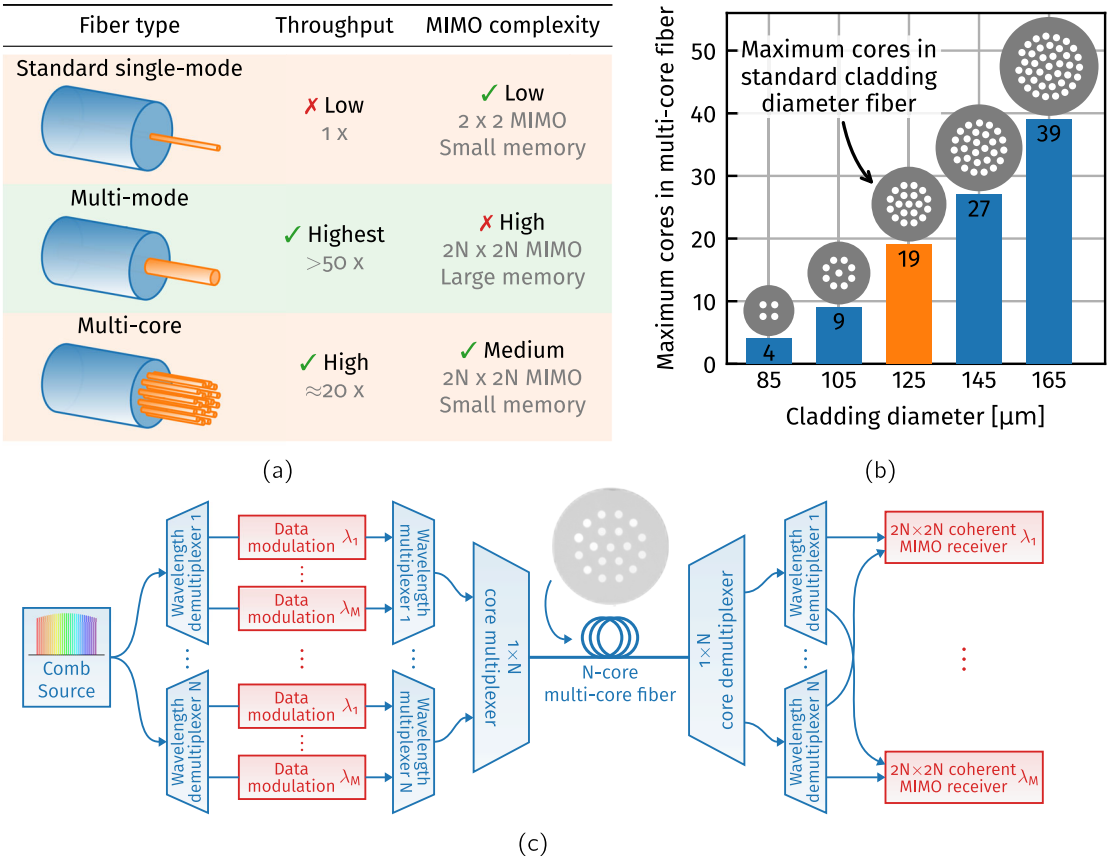

Fig. 1 | Multi-core fiber technology. a Comparison of standard SMF, multi-core, and MMF technologies, constrained to standard cladding diameter fibers. **b** Maximum number of cores in a multi-core fiber for different cladding diameters. **c** Schematic of a high-capacity multi-core-fiber-based transmission system. To address all the available spatial (N) and wavelength (M) channels of an MCF, $N \times M$ independent data signals are generated and multiplexed onto the MCF. At the receiver side, after demultiplexing the spatial and wavelength channels, M $2N \times 2N$ MIMO receivers reconstruct the transmitted data.

orthogonal spatial dimension of an optical fiber to increase the per-fiber capacity by orders of magnitude and, at the same time, reduce the cost-per-bit and power consumption through system integration, a necessity for the commercial deployment of such systems[9].

For SDM systems, novel fiber types must be designed and fabricated. Proposed fiber types are depicted in Fig. 1a and include coupled-core and weakly-coupled multi-core fibers (MCFs)[10,11], which provide additional spatial channels by housing multiple cores in a single shared cladding, and multi-mode fibers (MMFs)[12,13] adapt the fiber in such a way that multiple spatial modes are guided in a single core. Randomly-coupled MCFs, where the single-mode cores are arranged to maximize random coupling between cores, can offer a high spatial density while having lower transmission impairments compared to weakly coupled MCFs and MMFs[14,15].

Recently, research on SDM fibers has shifted towards fibers that maintain the current industry standard cladding diameter of 125 μm. Maintaining a standard cladding diameter is crucial, as the existing fiber plant is based on a 125 μm cladding diameter, and significant research and development have focused on improving manufacturing, yield, tooling, optical fiber connectorization, and deployment reliability around this cladding diameter. Previous fiber designs aiming to deliver maximum capacity have resulted in larger cladding diameters[16–18], but those fibers are increasingly difficult to handle, and for example, connect by fusion splicing. Furthermore, standard cladding diameter fibers are reported to have higher reliability and production yield in comparison to larger cladding diameter fibers[19–21]. Thus, maintaining the standard 125 μm cladding diameter is preferred.

Figure 1a compares the maximum data throughput and required receiver complexity of standard cladding diameter fibers for three fiber types. Specifically, the multiple-input multiple-output (MIMO) equalizer complexity is compared, as this equalizer compensates for the mixing and temporal delay between transmitted signals occurring during transmission in the fiber. As a SMF supports only a single spatial path, naturally, it has the lowest throughput. The temporal spread of the transmitted signal is only affected by polarization mode dispersion. Hence, only a relatively low-complexity 2×2 MIMO equalizer with a small temporal memory is required to undo the mixing between the two received polarizations and receive the transmitted data. While MMFs allow for the highest spatial density in a standard cladding diameter fiber, and up to 55 modes in a single core have been demonstrated in ref. 22, the MMF channel can have disadvantageous properties. These include a different per-mode attenuation resulting in mode-dependent loss (MDL) and a large temporal spread between the propagating modes[23], which requires a complex, large temporal memory $2N \times 2N$ MIMO equalizer, with N the number of orthogonal spatial paths, as it needs to undo both the mixing and delay between modes. For MCFs, however, the maximum number of cores in a weakly-coupled MCF is limited to around 4 for transmission in the C- and L-band to keep the inter-core crosstalk within acceptable limits and allow the use of conventional and standardized transceiver hardware[20,24]. When more cores are placed inside a single cladding whilst maintaining the standard cladding diameter, the inter-core crosstalk becomes non-negligible, and the data from all the cores has to be jointly processed to recover the transmitted data, requiring novel transceiver hardware. High-spatial-density randomly-coupled MCFs offer a lower MDL, smaller temporal spread of the propagating signal, and lower fiber nonlinearities compared to weakly coupled MCFs and MMFs[14]. Figure 1b shows the dependence of the maximum number of

https://doi.org/10.1038/s41467-025-59037-1

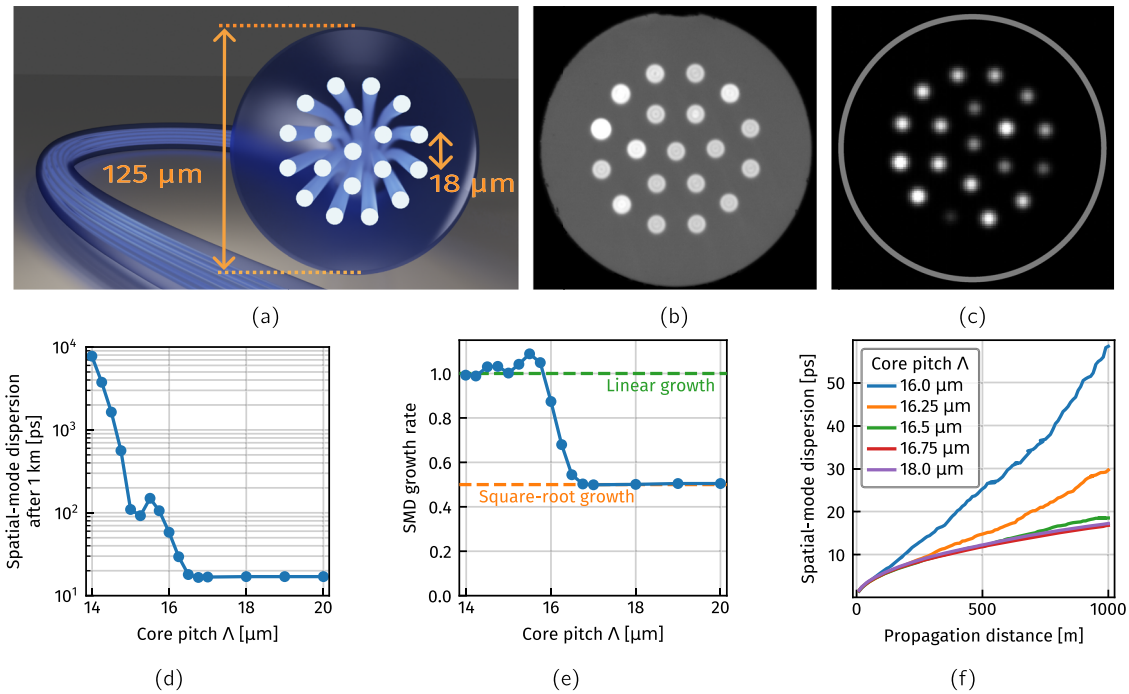

Fig. 2 | Design of the 19-core fiber. a Artist's impression of the cross-section of the 19-core fiber. **b** Micrograph of the cross-section of the 19-core fiber. **c** Infrared camera image of the output facet after 10 m of 19-core fiber when exciting the center core with 3 nm wide ASE centered at 1550 nm. The gray circle indicates the outer edge of the cladding. **d** Simulated spatial-mode-dispersion vs core pitch Λ. **e** Simulated spatial-mode-dispersion growth rate vs core pitch Λ. **f** Simulated spatial-mode-dispersion accumulation with distance.

cores in a randomly-coupled MCF on the cladding diameter. Here, we assumed a minimum core pitch of 18 μm and a sufficiently large distance between the outermost cores and the cladding edge to prevent higher losses on these cores. For a standard cladding diameter of 125 μm, 19 cores are approximately the maximum number of cores that can be packed in a single fiber. As the throughput is proportional to the number of cores, compared to an SMF, standard cladding diameter MCFs can achieve a throughput that is ≈20× higher. As for such fibers, the cores are placed close enough to each other for signals to couple between cores, a $2N \times 2N$ MIMO equalizer is needed. Figure 1c shows a schematic of an envisioned transmission system using a randomly-coupled MCF. Optical carriers are provided by an optical frequency comb and are modulated to generate $N \times M$ independent data signals. Here, M denotes the number of wavelength-division multiplexing (WDM) channels used in the system. The generated signals are multiplexed onto the MCF. On the receiver side, after core and wavelength demultiplexing, $M2N \times 2N$ coherent MIMO receivers are used to receive the transmitted data. Previous notable demonstrations of randomly-coupled MCFs include 3, 4, 7, and 12 core fibers[14,15,25–27].

In this work, we increase this core-count and present the design, fabrication, and characterization of a 19-core randomly-coupled MCF, which we employed in a transmission experiment to demonstrate a record-breaking data rate for a standard cladding diameter fiber[28]. The 63.5 km long fabricated fiber had a spatial-mode dispersion (SMD) coefficient of 10.8 ps/$\sqrt{\text{km}}$ at 1550 nm with a high uniformity over the C- and L-bands. While the fiber has the highest reported number of coupled cores, it has SMD values comparable to fibers with fewer cores[15]. A total data rate of 1.7 petabit/s was achieved by transmitting 381 wavelength channels × 19 cores × 24.5 GBaud 64-ary quadrature amplitude modulation (QAM) signals, the highest reported data rate for any standard cladding diameter multi-core fiber and more than an order of magnitude higher than is supported by currently operational SMF-based systems. These results highlight the strong potential of randomly-coupled MCFs in applications where high spatial density needs to be combined with high-quality transmission, such as submarine communication links or ultra-high-density interconnects.

Results

19-core fiber design and characterization

The randomly-coupled 19-core fiber was designed with 19 silica cores in a 125 μm cladding diameter, of which a schematic is shown in Fig. 2a with the cross-section of the fabricated fiber shown in the photograph in Fig. 2b. To ensure strong light confinement within the cores, each core was tailored to have an effective area of 62 μm^2. The cable cutoff wavelength for the higher-order modes corresponding to the linearly polarized (LP) LP_{11} modes was measured to be 1.36 μm. This potentially enables transmission over a wide bandwidth covering the S, C, and L wavelength bands from 1460 nm to 1625 nm. Figure 2d–f show the relationship between SMD, which is proportional to the temporal spread of the signal introduced by the MCF, and the core pitch Λ obtained by numerical simulations[29]. For simulations, a fiber bend radius of 0.17 m was assumed based on the average bend radius when spooling the fiber on a bobbin with a diameter of 0.17 m. Furthermore, a deterministic sinusoidal twist with a peak rate of 2 turns/m, random twist components with a standard deviation σ of 0.3 turns/$\sqrt{m}$, and a correlation length of 0.05 m were used. Figure 2d shows that the SMD after 1 km of propagation decreases exponentially when the core pitch Λ increases from 14 μm to 16.5 μm and evolves to an almost constant value between a core pitch of 16.75 μm to 20 μm. Figure 2e, f show that the threshold between the systematic coupling regime (associated with smaller Λ and a linear SMD growth) and the random coupling regime (larger Λ, square-root SMD growth) lies around $\Lambda = 16.5$ μm. Based on these simulations, a 63.5 km long piece of 19-core MCF was fabricated with a core pitch of 18 μm to enhance random mode mixing.

An infrared photograph of the output facet of a 10 m piece of the manufactured fiber is shown in Fig. 2c. At the input of the fiber, the center core was excited with a 3 nm wide amplified spontaneous emission (ASE) spectrum, and Fig. 2c qualitatively confirms strong coupling within the fiber after 10 m. The mode-averaged attenuation

https://doi.org/10.1038/s41467-025-59037-1

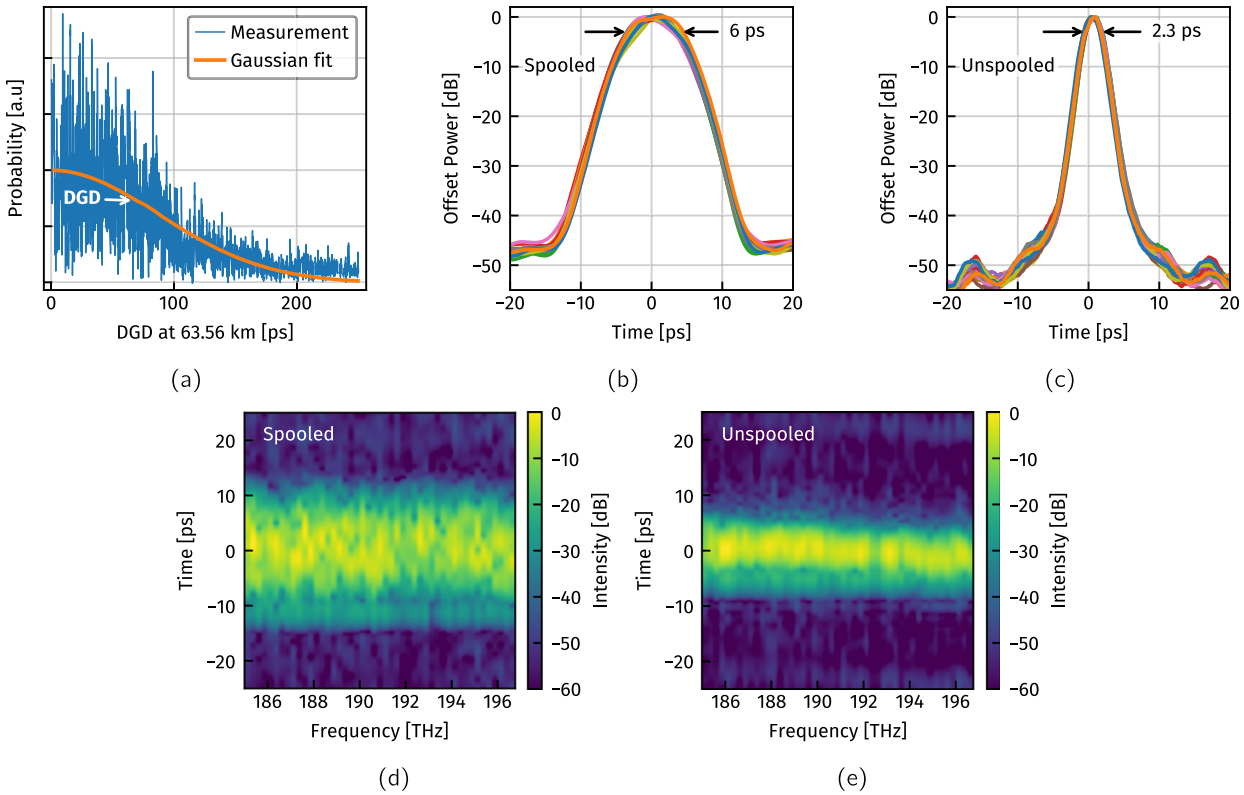

Fig. 3 | Characterization of the 19-core fiber. a DGD distribution of the fabricated 19-core fiber measured using the fixed analyzer method. **b**, **c** IIRs for 100 m of spooled and unspooled 19-core fiber. **d**, **e** Spectrograms for spooled and unspooled fiber, respectively.

and MDL at 1550 nm were measured to be 0.215 dB/km and 0.1 dB, respectively. The chromatic dispersion and chromatic dispersion slope at 1550 nm were 17.2 ps/(nm·km) and 0.055 ps/(nm^2 125·km), respectively, comparable to conventional SMFs[30]. The SMD coefficient was measured to be 10.8 ps/$\sqrt{\text{km}}$ (86.4 ps after 63.56 km), which was measured using the wavelength scanning (fixed analyzer) method[14] in a range from 1525 nm to 1575 nm. Figure 3a shows the differential group delay (DGD) distribution measured with the center core as input and output. The SMD coefficient of the fabricated MCF was slightly better than the above simulation results (17 ps/$\sqrt{\text{km}}$), indicating that the longitudinal deterministic and random perturbations on the fabricated fiber spool are stronger than the assumptions from the SMD simulation.

A 100 m long piece of 19-core MCF was characterized[31] using swept wavelength interferometry (SWI)[32,33]. Light from a frequency-swept laser was launched into the center core, and the Rayleigh backscattered signal was analyzed. Based on the power of the reflections, it was observed that after about 10 cm of propagation, the signal is fully randomly distributed across all 19 cores. The individual intensity impulse responses (IIRs) of all cores were obtained by measuring the swept laser light at the output of the MCF for every output core using a collimator. Figure 3b, c show the intensity of these impulse responses in the case of spooled (spool diameter = 16 cm) and unspooled fiber, for which the fiber was placed between two pieces of acoustic foam in an oval shape with dimensions of 0.5 m and 1 m. The individual IIRs perfectly overlap, indicating good uniformity between all cores. The SMD coefficient was calculated to be 4.9 ps/$\sqrt{\text{km}}$ 19.3 ps/$\sqrt{\text{km}}$ for the unspooled and spooled case, respectively. This reduction in SMD coefficient when unspooling, i.e., increasing the fiber bend radius, agrees with previous SMD measurements on other MCFs[34]. SMD coefficient for the spooled fiber was higher compared to the 10.8 ps/$\sqrt{\text{km}}$ measured earlier. However, the 100 m piece of fiber was spooled around a bobbin with a smaller radius, which increased the SMD. The lower SMD measured on the unspooled fiber gives a more realistic approximation of the SMD when the fiber is to be field-deployed. Furthermore, Fig. 3d, e show the spectrogram of the IIR of a single core, confirming that the IIR is stable over frequencies across the C- and L-band.

19-core 3D-inscribed core-multiplexer

Custom-designed core-multiplexers were fabricated to couple light from 19 SMFs into the 19-core MCF. The core multiplexers were based on 3D integrated photonics[35–37], where for this multiplexer, a boro-aluminosilicate glass substrate was modified using femtosecond laser pulses to form the waveguide structure shown in Fig. 4a. Using femtosecond laser pulses, this technique enables a highly localized and permanent modification to the refractive index of the glass, allowing the inscription of waveguides that follow a three-dimensional trajectory. The waveguides on one side of the multiplexer were placed onto a linear array compatible with commercial fiber arrays of 127 μm pitch, while the waveguides on the other side of the multiplexer were arranged into the core layout of the 19-core MCF. To achieve the best possible overlap and thus the lowest losses between the MCF and 3D waveguide chips, the exact positions of each core on both ends of the MCF spool were measured and aligned using an optical microscope assisted by machine vision. The SMF array and MCF were butt-coupled to the multiplexer and affixed using UV curing adhesive after optimizing the alignment in all 6 degrees of freedom on either side. The interfaces between the fibers and the waveguide chip were polished at an angle of 8° to minimize the return loss. Figure 4b shows photographs of the fabricated multiplexer and the multiplexer assembly. The size of the glass multiplexer is in the order of 13 × 5 × 2 mm, and the multiplexer assembly has 19 SMF pigtails and a 19-core fiber pigtail, which can be fusion-spliced to the 19-core MCF spool. Two core-multiplexers were fabricated to be used as fan-in and fan-out devices, of which the insertion loss (IL) is characterized in Fig. 4c. As the 19-core

https://doi.org/10.1038/s41467-025-59037-1

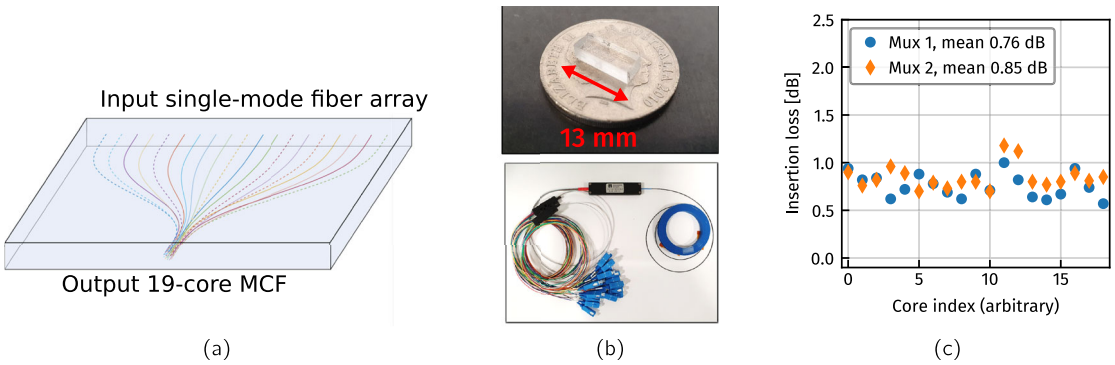

Fig. 4 | 19-core 3D-inscribed core multiplexer. a Schematic of the glass-inscribed core multiplexer, which converts 19 single-mode inputs into the correct spatial layout to address the 19-core fiber. **b** A photograph of the fabricated core multiplexer on an Australian dollar coin to depict scale and the pigtailed and connectorized core multiplexer assembly. **c** Measured per-input-core IL of the core multiplexers, indicating uniform IL for all cores.

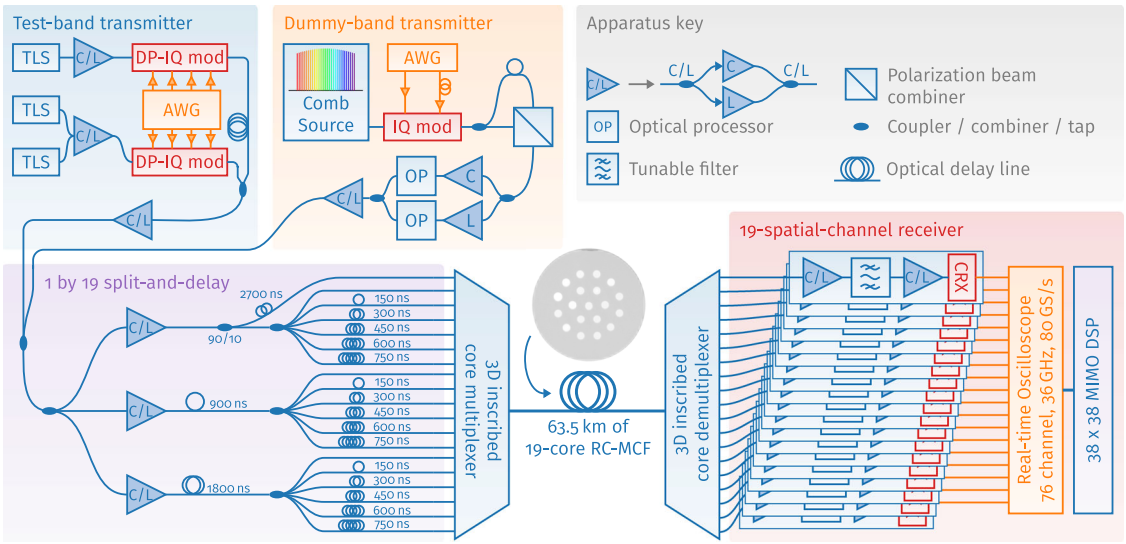

Fig. 5 | Laboratory setup for data transmission over a 19-core fiber. Three hundred eighty-one wavelength channels were generated and modulated with dual-polarization 64-QAM signals. To address all 19 cores, all 381 channels were split and delayed to generate 19 decorrelated copies, which were transmitted over the 19-core fiber. At the receiver, a 38 × 38 coherent MIMO receiver was used to undo mixing between the spatial channels and recover the transmitted signal.

MCF does not have an alignment marker, the assigned core index is arbitrary. A uniform IL across all the cores was observed, and the average IL was 0.8 dB, including the connectors.

Transmission channel characterization and data transmission

To assess the data transmission capabilities of the 19-core MCF, a laboratory transmission setup was assembled as summarized in Fig. 5 and explained in further detail in the "Methods" section. In short, the setup comprises a 381 channel WDM transmitter that transmits polarization-multiplexed 64QAM signals, a 3D-inscribed core multiplexer, 63.5 km of 19-core MCF, a core demultiplexer, and a 38 × 38 coherent MIMO receiver. Figure 6a shows the IIR of a wavelength channel at 1550 nm calculated from the taps of the MIMO equalizer. The IIR has a Gaussian shape[38], and the standard deviation σ is 44 ps. This corresponds to only 2.2 equalizer taps at a symbol rate of 24.5 GBaud. This standard deviation is in line with the SMD (which is 2σ of the IIR) measurements from the previous section and is comparable to SMD values reported previously for randomly-coupled MCFs with fewer cores[27]. The wavelength-dependence of the standard deviation of the IIR is investigated in Fig. 6b. The variation across an almost 80 nm wide spectral band covering the C- and L-bands is within 10 ps, indicating high spectral uniformity of the SMD. Figure 6c shows the coupling matrix obtained from the MIMO equalizer taps for the wavelength channel at 1550 nm. Strong coupling between all the cores is observed, as is evident from the absence of clustering, which would appear if only a subset of cores were strongly coupled. Finally, the data transmission capabilities of the 19-core MCF are demonstrated by calculating the data rates for all the 381 wavelength channels, which are shown in Fig. 6d. Both the data rate based on generalized mutual information (GMI)[39] and the data rate after applying a decoding scheme[40] mainly based on the DVB-S2 standard[41] are calculated. The data rates per wavelength channel in the C-band were approximately 5 terabit/s and between 3 terabit/s to 5 terabit/s in the L-band. The reduced performance for higher L-band wavelength channels is mainly attributed to a higher erbium-doped fiber amplifier (EDFA) noise figure for those wavelengths. The sudden drop in performance compared to neighboring channels for a select number of wavelength channels is attributed to wavelength filters in the coherent receivers, which were not correctly tuned, and not to the transmission fiber itself. The total data rates, the sum of the per-wavelength-channel data rates, were calculated to be 1.7 petabit/s and 1.8 petabit/s, after the decoding scheme and based on GMI, respectively. This data rate is the highest reported for any multi-core fiber with a standard 125 μm cladding diameter.

https://doi.org/10.1038/s41467-025-59037-1

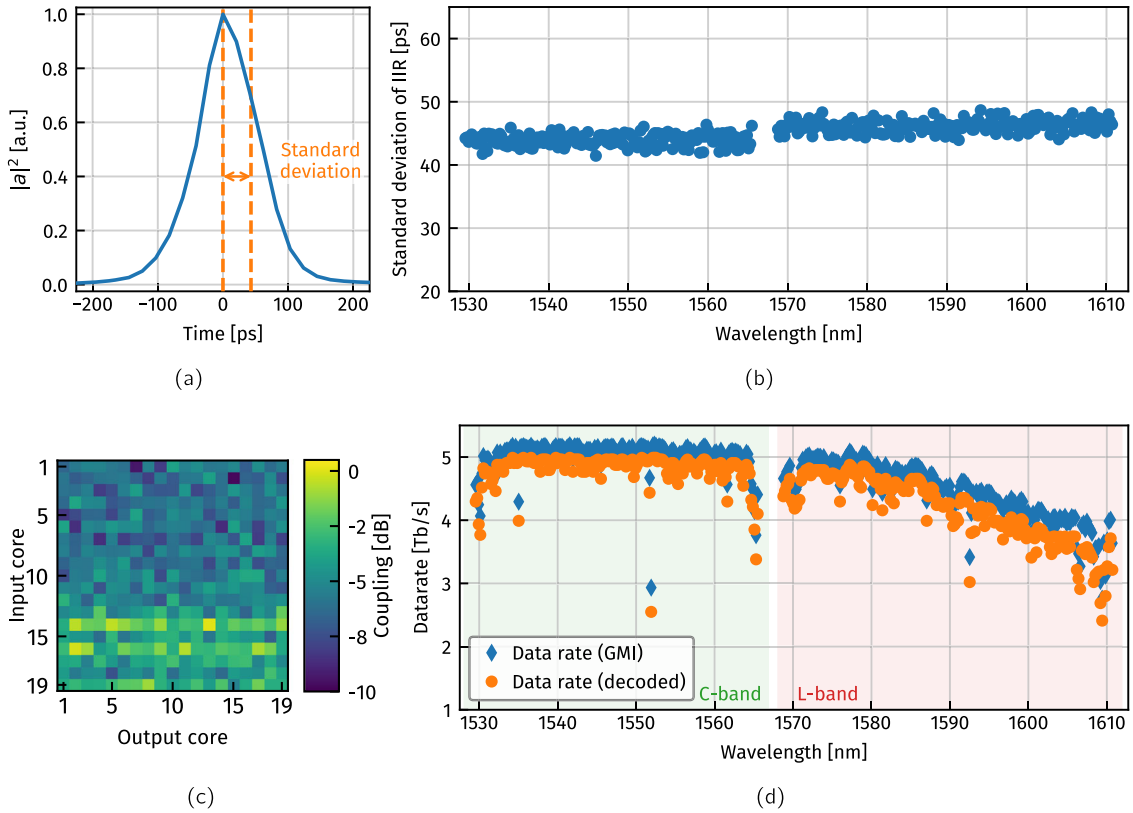

Fig. 6 | Transmission channel characteristics and data transmission results. a IIR of a channel at 1550 nm. **b** Standard deviation of the IIR of all the 381 measured wavelength channels. **c** Coupling matrix for a channel at 1550 nm confirming good coupling between all 19 cores. **d** Measured data rates of all the 381 wavelength channels.

Discussion

Next-generation SDM fibers will most likely maintain a cladding diameter of 125 μm, the current industry standard, for deployment and reliability reasons. Randomly-coupled MCFs offer a high spatial information density, yet with lower transmission impairments than weakly coupled MCFs and MMFs. Given the constraint on the cladding diameter, the maximum number of cores that can be accommodated in a randomly-coupled MCF with a standard cladding diameter of 125 μm is nineteen.

We designed a 19-core randomly-coupled MCF and optimized the design to ensure low SMD, which is key to reducing the system complexity. The 19-core randomly-coupled MCF was fabricated and characterized, and we demonstrated its data transmission capabilities by performing a WDM transmission experiment. The designed fiber had the maximum number of spatial channels supported in a standard cladding diameter multi-core fiber. The fabricated fiber had a length of 63.5 km and an SMD coefficient of 4.9 ps/$\sqrt{\text{km}}$ when unspooled. 3D-inscribed glass core-multiplexers were fabricated to couple in and out of the 19-core MCF with a low IL (<0.8 dB). This allowed the transmission of 1.7 petabit/s net data rate over 63.5 km of 19-core randomly-coupled MCF, the highest data rate reported for any coupled-core MCF and any standard cladding diameter MCF. This data rate can be further increased by also transmitting data signals in the optical S-band. Recently, 3.56 petabit/s transmission has been demonstrated in a 55-mode standard cladding diameter MMF[42]. While the total throughput was higher, due to MDL, the per-spatial-channel throughput was reduced in this MMF. Moreover, while in this work we transmitted over a five times longer distance compared to the MMF experiment, the temporal spread introduced by the MCF was more than one order of magnitude smaller, significantly reducing the receiver complexity.

These results emphasize the strong potential of coupled-core MCF in combination with MIMO digital signal processing for transmission links where high spatial density and high-quality transmission channels are required. Such applications could be found in high-capacity data-center interconnects or, given recent advances in multi-core amplifier technology, they can be found in long-haul submarine links.

Methods

Experimental implementation of 19-core transmitter

A schematic of the implemented transmitter setup can be found in Fig. 5. The transmitted signal consisted of a high-quality test band, which was used for performance evaluation, sliding over a dummy band. For the three-channel test-band, three tunable laser sources (TLSs) with a nominal linewidth below 10 kHz were amplified and modulated in two dual-polarization IQ-modulators (DP-IQMs). To amplify signals spanning both the optical C- and L-bands, C- and L-band EDFAs were combined with band-splitters/combiners, as seen in the inset in Fig. 5. The DP-IQMs were driven by a 4-channel 49 GS/s arbitrary-waveform generator (AWG) that was programmed to produce 24.5 GBaud (DP) 64-ary quadrature amplitude modulation (QAM) signals filtered with a RRC filter with a roll-off of 1% and pre-compensated for electrical bandwidth limitations. A single optical frequency comb[43] generated a wideband comb of laser lines with a spacing of 25 GHz, producing the tones for the WDM dummy channel band. These were modulated in a single-polarization IQ-modulator followed by a polarization-emulation stage and a spectral flattening stage employing programmable optical processors (OPs). In the absence of 19 such systems, the test- and dummy-band were combined using a power coupler, while OPs carved a notch around the test-band spectrum in the dummy-band, and connected to a split-and-delay stage. There, the signal was amplified and split, and delayed with increments of 150 ns to generate 19 decorrelated copies. The signals were amplified to 21 dBm per core, connected to the core-multiplexer, and transmitted over the 19-core MCF.

Experimental implementation of the receiver

The output of the 19-core MCF was connected to a core-demultiplexer. The outputs of the demultiplexer were received by a 19-channel SDM receiver, which mainly consisted of a two-stage EDFA-based amplifier with an optical bandpass filter in between to select the wavelength channel under test and 19 coherent receivers that shared the same local oscillator (LO), which had a nominal linewidth below 60 kHz. The electrical signals were digitized by a 76-channel equally configured real-time oscilloscope with a 36 GHz bandwidth, sampling at 80 GS/s. Offline digital signal processing (DSP) consisted mainly of a 38×38 MIMO equalizer with 81 half-symbol-duration-spaced taps, which were initialized in a data-aided least mean squares (LMS) mode before switching to a decision-directed LMS mode for signal performance estimation. Inside the equalizer, a decision-directed phase recovery algorithm[44] was also running.

Data rate estimation

To assess the quality of the received signal, data rates are calculated using both GMI[39] and the data rate after a decoding scheme. The decoding scheme was similar to the one from refs. 40,45. For both GMI and decoding, interleaving was assumed over time and spatial modes, resulting in spatial super-channels. Due to interleaving, the channel was assumed to be memoryless. GMI was used to estimate the maximum data rate assuming ideal bit-interleaved coded modulation (BICM) combined with optimal soft-decision forward error correction (FEC), while a more realistic estimate of the maximum data rate was given by the implemented decoding scheme. This scheme used a Monte Carlo approach to estimate the achievable data rate. Random binary patterns were generated using and encoded by low-density parity-checks (LDPCs) with various rates from the ref. 41 standard. Code-rate puncturing was used to obtain a code-rate granularity of 0.01. Bits were mapped to symbols, and matching symbols were selected randomly from the experimentally received symbol streams from all the modes. The code rate was changed to achieve a bit error rate (BER) below 5×10^{-5} with an additional hard-decision outer FEC code with 1% overhead to eliminate remaining bit errors[46]. Approximately 5×10^6 bits were used in the coding scheme to obtain sufficient error statistics. The data rate after decoding was obtained by removing the overhead of the inner and outer FEC from the gross data rate. The decoding scheme was applied on a per-capture basis, resulting in an optimized code rate for every wavelength channel.

Data availability

The data that support the findings of this study are available from the corresponding author upon reasonable request. Source data for Figs. 1–6 are provided with the paper. Source data are provided with this paper.

References

1. Agrawal, G. P. Optical communication: its history and recent progress. In *Optics in Our Time* (eds. Al-Amri, M. D., El-Gomati, M. & Zubairy, M. S.) 177–199 (Springer International Publishing, 2016). https://doi.org/10.1007/978-3-319-31903-2_8.
2. Cisco Annual Internet Report. *Cisco Annual Internet Report White Paper* (CISCO, 2018–2023).
3. Essiambre, R.-J. & Tkach, R. W. Capacity trends and limits of optical communication networks. *Proc. IEEE* **100**, 1035–1055 (2012).
4. Winzer, P. J., Neilson, D. T. & Chraplyvy, A. R. Fiber-optic transmission and networking: the previous 20 and the next 20 years [Invited]. *Optics Express* **26**, 24190 (2018).
5. Shtaif, M., Antonelli, C., Mecozzi, A. & Chen, X. Challenges in estimating the information capacity of the fiber-optic channel. *Proc. IEEE* **110**, 1655–1678 (2022).
6. Soma, D. et al. *25-THz O + S + C + L + U − B and Digital Coherent DWDM Transmission Using a Deployed Fibre-Optic Cable. Th.C.2.2* (IEEE, 2023).
7. Puttnam, B. J. et al. 402 Tb/s GMI data-rate OESCLU-band Transmission. In *2024 Optical Fiber Communications Conference and Exhibition (OFC)* 1–3 (OFC, 2024); https://ieeexplore.ieee.org/document/10527148.
8. Puttnam, B. J., Rademacher, G. & Luís, R. S. Space-division multiplexing for optical fiber communications. *Optica* **8**, 1186 (2021).
9. Winzer, P. J. & Neilson, D. T. From scaling disparities to integrated parallelism: a decathlon for a decade. *J. Lightwave Technol.* **35**, 1099–1115 (2017).
10. Saitoh, K. & Matsuo, S. Multicore fiber technology. *J. Lightwave Technol.* **34**, 55–66 (2016).
11. Li, M.-J. & Hayashi, T. Advances in low-loss, large-area, and multicore fibers. In *Optical Fiber Telecommunications VII* 3–50 (Elsevier, 2020). https://linkinghub.elsevier.com/retrieve/pii/B9780128165027000014.
12. Sillard, P. Few-mode fibers for space division multiplexing. In *2016 Optical Fiber Communications Conference and Exhibition (OFC)* 1–53 (Optica, 2016).
13. Sillard, P. et al. Few-mode fiber technology, deployments, and systems. *Proc. IEEE* **110**, 1804–1820 (2022).
14. Hayashi, T. et al. Randomly-coupled multi-core fiber technology. *Proc. IEEE* **110**, 1786–1803 (2022).
15. Ryf, R. et al. Coupled-core transmission over 7-core fiber. In *2019 Optical Fiber Communications Conference and Exhibition (OFC)* 1–3 (IEEE, 2019).
16. Rademacher, G. et al. Highly spectral efficient C + L-band transmission over a 38-core-3-mode fiber. *J. Lightwave Technol.* **39**, 1048–1055 (2021).
17. Soma, D. et al. 2.05 Peta-bit/s super-nyquist-WDM SDM transmission using 9.8-km 6-mode 19-core fiber in full C band. In *2015 European Conference on Optical Communication (ECOC)* 1–3 (ECOC, 2015); https://ieeexplore.ieee.org/document/7341686.
18. Puttnam, B. J. et al. 22.9 Pb/s data-rate by extreme space-wavelength multiplexing. Th.C.2.1. In *49th European Conference on Optical Communications* (ECOC, 2023).
19. Hayashi, T. et al. 125-μm-cladding eight-core multi-core fiber realizing ultra-high-density cable suitable for O-band short-reach optical interconnects. *J. Lightwave Technol.* **34**, 85–92 (2016).
20. Matsui, T., Pondillo, P. L. & Nakajima, K. Weakly coupled multicore fiber technology, deployment, and systems. *Proc. IEEE* **110**, 1772–1785 (2022).
21. Matsuo, S. et al. High-spatial-multiplicity multicore fibers for future dense space-division-multiplexing systems. *J. Lightwave Technol.* **34**, 1464–1475 (2016).
22. Rademacher, G. et al. 1.53 Peta-bit/s C-band transmission in a 55-mode fiber. In *2022 European Conference on Optical Communication* 1–4 (ECOC, 2022).
23. Sillard, P. et al. 55-Spatial-mode fiber for space division multiplexing. In *2023 Optical Fiber Communications Conference and Exhibition* 1–3 (OFC, 2023).
24. Mukasa, K. et al. Uncoupled 6-core fibers with a standard 125-um cladding, ITU-T G.652 optical properties, and low XT. In *2023 Optical Fiber Communications Conference and Exhibition (OFC)* 1–3 (IEEE, 2023).
25. Rademacher, G. et al. 172 Tb/s C + L band transmission over 2040 km strongly coupled 3-core fiber. In *2020 Optical Fiber Communications Conference and Exhibition (OFC)* 1–3 (Optica Publishing Group, 2020).
26. Hayashi, T., Tamura, Y., Hasegawa, T. & Taru, T. Record-low spatial mode dispersion and ultra-low loss coupled multi-core fiber for ultra-long-haul transmission. *J. Lightwave Technol.* **35**, 450–457 (2017).

27. Sakamoto, T. et al. Twisting-rate-controlled 125 um cladding randomly coupled single-mode 12-core fiber. *J. Lightwave Technol.* **36**, 325–330 (2018).
28. Rademacher, G. et al. Randomly coupled 19-core multi-core fiber with standard cladding diameter. In *OFC 2023*, Th4A.4 (Institute of Electrical and Electronics Engineers, 2023).
29. Hayashi, T., Nagashima, T., Muramoto, T., Sato, F. & Nakanishi, T. Spatial mode dispersion suppressed randomly-coupled multi-core fiber in straightened loose-tube cable. In *2019 Optical Fiber Communications Conference and Exhibition (OFC)* 1–3 (Optica Publishing Group, 2019).
30. Corning® SMF-28e+® Optical Fiber. *CORNING* (2021). https://www.corning.com/media/worldwide/coc/documents/Fiber/PI-1463-AEN.pdf.
31. Dallachiesa, L. et al. Broadband characterization of randomly coupled 19-core multicore fiber. In *2024 Optical Fiber Communications Conference and Exhibition (OFC)* 1–3 (Institute of Electrical and Electronics Engineers, 2024); https://ieeexplore.ieee.org/document/10526718.
32. Fontaine, N. K. et al. Characterization of space-division multiplexing systems using a swept-wavelength interferometer. In *Optical Fiber Communication Conference/National Fiber Optic Engineers Conference 2013*, OW1K.2 (OSA, 2013); https://opg.optica.org/abstract.cfm?URI=OFC-2013-OW1K.2.
33. Rommel, S. et al. Few-mode fiber, splice and SDM component characterization by spatially-diverse optical vector network analysis. *Optics Express* **25**, 22347 (2017).
34. Hayashi, T. et al. Field-deployed multi-core fiber testbed. In *2019 24th OptoElectronics and Communications Conference (OECC) and 2019 International Conference on Photonics in Switching and Computing (PSC)* 1–3 (PSC, 2019); https://ieeexplore.ieee.org/abstract/document/8818058.
35. Thomson, R. R. et al. *Ultrafast-Laser Inscription of a Three Dimensional Fan-Out Device for Multicore Fiber Coupling Applications* (Optica Publishing Group, 2007).
36. Gross, S. & Withford, M. J. Ultrafast-laser-inscribed 3D integrated photonics: challenges and emerging applications. *Nanophotonics* **4**, 332–352 (2015).
37. Thomson, R. R. et al. Ultrafast laser inscription of a 121-waveguide fan-out for astrophotonics. *Optics Lett.* **37**, 2331–2333 (2012).
38. Ryf, R. & Antonelli, C. Space-division multiplexing. In *Springer Handbook of Optical Networks*, Springer Handbooks (eds. Mukherjee, B., Tomkos, I., Tornatore, M., Winzer, P. & Zhao, Y.) 353–393 (Springer International Publishing, 2020); https://doi.org/10.1007/978-3-030-16250-4_10.
39. Alvarado, A., Agrell, E., Lavery, D., Maher, R. & Bayvel, P. Replacing the soft-decision FEC limit paradigm in the design of optical communication systems. *J. Lightwave Technol.* **34**, 707–721 (2016).
40. Rademacher, G. et al. High capacity transmission with few-mode fibers. *J. Lightwave Technol.* **37**, 425–432 (2019).
41. Digital Video Broadcasting (DVB). *Second Generation Framing Structure, Channel Coding and Modulation Systems for Broadcasting, Interactive Services, News Gathering and Other Broadband Satellite Applications; Part 1: DVB-S2* (ETSI, 2014).
42. Rademacher, G. et al. *3.56 Peta-bit/s C + L Band Transmission Over a 55-Mode Multi-Mode Fiber. We.A.1.1* (Institution of Engineering and Technology, 2023).
43. Kuo, B. P.-P. et al. Wideband parametric frequency comb as coherent optical carrier. *J. Lightwave Technol.* **31**, 3414–3419 (2013).
44. Pfau, T., Hoffmann, S. & Noe, R. Hardware-efficient coherent digital receiver concept with feedforward carrier recovery for M-QAM constellations. *J. Lightwave Technol.* **27**, 989–999 (2009).
45. Rademacher, G. et al. Peta-bit-per-second optical communications system using a standard cladding diameter 15-mode fiber. *Nat. Commun.* **12**, 4238 (2021).
46. Millar, D. S. et al. Design of a 1 Tb/s superchannel coherent receiver. *J. Lightwave Technol.* **34**, 1453–1463 (2016).

Acknowledgements

The work of M.v.d.H. and C.O. was partly supported by the TU/e-KPN flagship Smart Two project and the PhotonDelta Dutch National Growth Funds for Photonics. G.D.S. and C.A. were supported by the Italian Government through the project INCIPICT.

Author contributions

M.v.d.H. and G.R. designed and carried out the data transmission experiment and analyzed the data with support from R.S.L., B.J.P., and G.D.S. T.H., A.I., and T.N. designed, fabricated, and performed initial characterization measurements on the multi-core fiber. S.G., A.R.-A., and M.J.W. designed and fabricated the core multiplexer devices. L.D., N.K.F., R.R., M.M., and H.C. performed further swept-wavelength interferometry measurements on the multi-core fiber. J.S., C.A., C.O., and H.F. supervised the overall experiments and process.

Competing interests

The authors declare no competing interests.

Additional information

Supplementary information The online version contains supplementary material available at https://doi.org/10.1038/s41467-025-59037-1.

Correspondence and requests for materials should be addressed to Menno van den Hout.

Peer review information *Nature Communications* thanks Xin Chen and the other anonymous reviewer(s) for their contribution to the peer review of this work. A peer review file is available.